Original Paper

Elasto-Plastic Behavior of Compression Members Laterally-Braced at an Intermediate Point

Hidekuni FUKAO, Shosuke MORINO, Jun KAWAGUCHI and Shizuko KUWADA†
(Department of Architecture)

(Received September 16, 1999)

Abstract

A total of 38 specimens of the eccentrically-loaded compression members elastically-braced at an intermediate point were tested, and the elasto-plastic behavior was analyzed by the method which sought for the deflected shape satisfying the equilibrium at the subdivision points along the member length. The effect of experimental parameters, i.e., normalized slenderness ratio, position of the brace and brace stiffness on the behavior of deflection reversal, bracing force ratio and maximum strength were investigated.

Keywords: Compression member, Buckling, Bracing force, Bracing stiffness

1. Introduction

In the design of a steel compression member, it is sometimes braced at an arbitrary intermediate point to increase the strength by decreasing the effective buckling length. A number of researches on the bracing requirements for the compression member with the intermediate brace have been reported[1-6], and the elasto-plastic behavior was experimentally investigated[2,4]. However, in most cases, only the case of the brace placed at the center of the member was considered. Consequently, the bracing requirements derived were rather too moderate. For example, the conventional design often assumes the force in the brace to be equal to 2% of the force acting on the compression member[7], but the bracing force well exceeds 2% in the case that the initial crookedness is large, and/or the intermediate brace cannot be arranged at the center. In addition, the research in the past have not fully clarified the phenomenon of the deflection reversal involved in the behavior of the laterally-braced compression member, that is, the deflected configuration of a initially-crooked compression member suddenly shifts from the first mode to the second[8]. There has been no information available on its effect on the bracing requirements. In order to clarify those problems mentioned, experimental investigation was carried out for the behavior of eccentrically-loaded compression members which were elastically-braced at an intermediate point other than the center.

† ANDO Structural Engineers

The paper first introduces the results of tests, and then discusses the elasto-plastic behavior including the deflection reversal, and the effects of the position and the stiffness of the elastic brace on the maximum strength of the compression member and the bracing force.

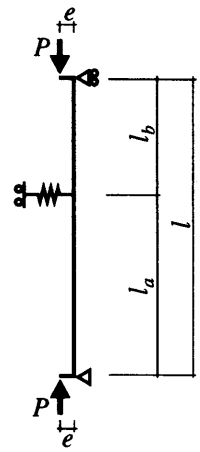

Fig. 1 Test Condition

2. Experimental investigation

2.1 Outline of the test

Eccentrically-loaded steel compression members were tested, which were elastically braced at an intermediate point, and the maximum load-carrying capacity, the force generated in the elastic brace and the deflection reversal were investigated. Figure 1 shows a schematic view of the test. The following parameters were varied in the tests: i) normalized slenderness ratio Λ of the compression member (Λ = 1.0, 1.5, 2.0 and actual slenderness ratio λ = 240), ii) position of the lateral brace l_b / l (at the distance equal to 1/2, 1/3, or 1/4 of the member length from the upper end support), and iii) stiffness parameter k of the lateral brace (k = 1, 3, and 5). Normalized slenderness ratio Λ is defined as $\Lambda = (l/i)(\sqrt{\sigma_y/E})/\pi$, where l = member length, i = radius of gyration of the member cross section, and σ_y and E = yield stress and elastic modulus of the member material, respectively. The stiffness parameter k is the ratio of the elastic stiffness of the lateral brace used in the test to the stiffness K_0 defined below:

$$K_0 = \frac{l_a + l_b}{l_a l_b} P_{cr} \tag{1}$$

where

$$P_{cr} = \frac{\pi^2 EI}{l_a^2} \qquad \text{for} \quad \Lambda_a \geq 1.0 \tag{2a}$$

$$P_{cr} = P_y \qquad \text{for} \quad \Lambda_a < 1.0 \tag{2b}$$

and P_y and I = yield axial strength and moment of inertia of the member cross section, l_a and l_b = length of the longer and shorter segments of the member divided by the lateral brace, as shown in Fig. 1, and normalized slenderness ratio Λ_a is calculated for the length l_a. The stiffness K_0 with P_{cr} given by Eq. (2a) is the minimum stiffness required for the elastic buckling strength of a centrally-loaded compression member which is braced at l_a to become Euler's buckling strength of a member with length equal to l_a given by Eq. (2a). The same eccentricity $e = i/20 + l/500$ was given at both ends of the member.

2.2 Test setup

Figure 2 shows the test setup. The compression load was applied to the specimen through the knife edges by the hydraulic jack, and it was measured by the load cell. The elastic lateral brace consisted of a simply-supported round bar A of high-strength steel used for prestressing tendon and a round bar B of mild steel connecting the center of the simply-supported bar A and the specimen. The stiffness of the lateral brace was therefore mainly given by the flexural stiffness of the bar A and the tensile stiffness of the bar B. The lateral deflections and the

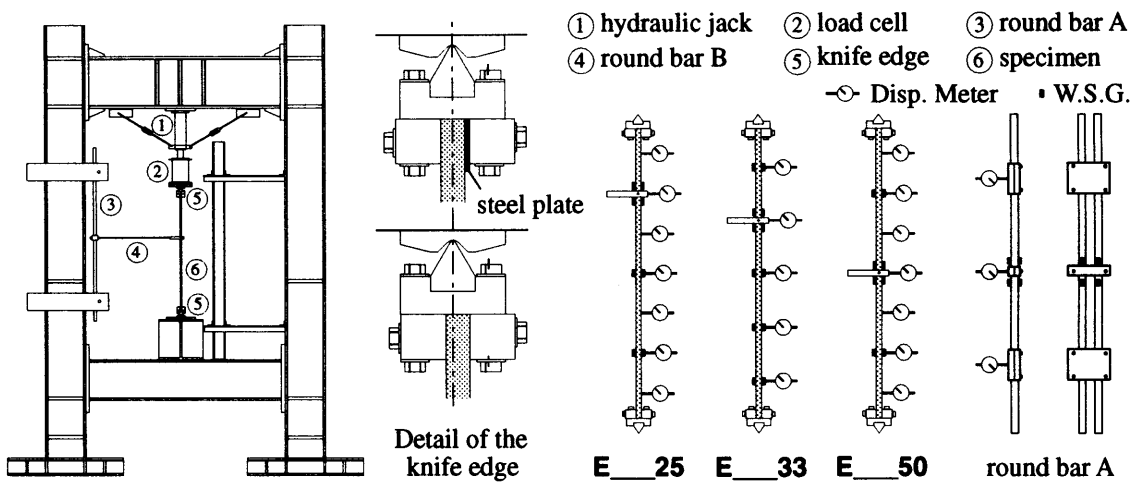

Fig. 2 Test Setup

strains were measured at several points along the length of the specimen shown in Fig. 2 by displacement meters and the wire strain gauges, respectively. The strains of the bars A and B were also measured, which were used to calculate the bracing force.

The position of the compression load was first aligned according to the strain measurements with a steel plate inserted between the specimen and the end fixture as shown in Fig. 2, and then the eccentricity was set by removing the steel plate. The thickness of the plate was adjusted to a required value equal to the eccentricity.

2.3 Specimen

The specimen was a flat bar with the size of 38x16 mm. Table 1 shows the name of the specimen and the

Table 1 Experimental Variables

specimen	eccentricity e	slenderness ratio Λ	support position l_b/l	stiffness parameter k	specimen	eccentricity e	slenderness ratio Λ	support position l_b/l	stiffness parameter k
E10125				1	**E20125**				1
E10325			0.25	3	**E20325**			0.25	3
E10525				5	**E20525**				5
E10133				1	**E20133**				1
E10333		1.0	0.33	3	**E20333**		2.0	0.33	3
E10533				5	**E20533**				5
E10150				1	**E20150**				1
E10350			0.50	3	**E20350**			0.50	3
E10150	$\frac{i}{20}+\frac{l}{500}$			5	**E20550**	$\frac{i}{20}+\frac{l}{500}$			5
E15125				1	**E24125**				1
E15325			0.25	3	**E24325**			0.25	3
E15525				5	**E24525**				5
E15133				1	**E24133**				1
E15333		1.5	0.33	3	**E24333**		240	0.33	3
E15533				5	**E24533**				5
E15150				1	**E24150**				1
E15350			0.50	3	**E24350**			0.50	3
E15550				5	**E24550**				5
E24525'		240	0.25	5	**E24350'**		240	0.50	3

E15325
- support position : $l_b/l = 0.25 \rightarrow$ **25**, $l_b/l = 0.33 \rightarrow$ **33**, $l_b/l = 0.50 \rightarrow$ **50**
- stiffness parameter : $k = 1 \rightarrow$ **1**, $k = 3 \rightarrow$ **3**, $k = 5 \rightarrow$ **5**
- slenderness ratio : $\Lambda = 1.0 \rightarrow$ **10**, $\Lambda = 1.5 \rightarrow$ **15**, $\Lambda = 2.0 \rightarrow$ **20**, $\lambda = 240 \rightarrow$ **24**

Table 2 Material Properties (Compression members)

material	A	B	C
yield stress σ_y [N/mm^2]	280.38	283.71	596.32
tensile strength σ_u [N/mm^2]	429.14	436.20	624.22
elongation [%]	31.98	30.57	24.28
elastic modulus E [kN/mm^2]	204.90	207.72	211.20

Table 3 Material Properties (Bracing member)

material	D	E
diameter 1 [mm]	26.017	32.017
diameter 2 [mm]	25.983	31.983
elastic modulus E [kN/mm^2]	211.61	221.26

values of the experimental variables. The first two digits of the five digit number of the specimen name indicate the value of Λ, the next one digit the value of k, and the last two digits the value of l_b/l. For example, **E15325** is the specimen with the values of Λ, k, and l_b/l equal to 1.5, 3, and 0.25, respectively. The material properties shown in Table 2 were obtained from the tensile tests of the bars with the same size as the ones used for the compression tests, a typical stress-strain curve being shown in Fig. 3. Two different materials were used for the simply-supported bar A in the bracing system, whose properties are listed in Table 3.

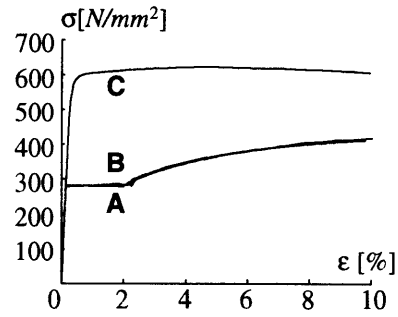

Fig. 3 Stress-Strain Relation

Table 4 shows measured dimensions of the specimens and the values of the stiffness parameter k_e, which were calculated from the displacement at the connection between the bracing bar B and the specimen and the bracing force obtained from the strain gauge data of the bar A (see Fig. 2). This displacement included the deformation of not only the bars A and B but also the connecting devices, and thus the values of k_e are somewhat smaller than the specified values listed in Table 1.

3. Analytical investigation

3.1 Model for analysis

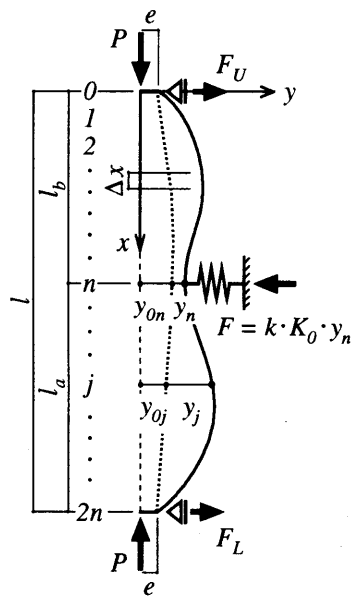

Fig. 4 Model for Analysis

Figure 4 shows the model of a simply-supported compression member of length l, which is intermediately braced at the distance l_b from the upper end. The brace is shown by an elastic spring with spring constant $K = (k \cdot K_0)$. The axial load P is applied with the eccentricity e at both ends, and the deflection y is generated by the axial load, in addition to the initial deflection y_0. The vertical reaction forces at the upper and the lower supports and at the spring are denoted by F_U, F_L and F, respectively.

3.2 Integration Procedure

The load-deflection relation of the braced member shown in Fig. 4 was analyzed by a conventional numerical integration scheme, dividing each of the upper and lower portions separated at the brace into n segments. The equilibrium equation of jth segment is written as follows, referring to Fig. 4:

$$0 \le j < n \qquad M_j = -P(y_{0j} + y_j) + F_U \, j \Delta x_U \tag{3}$$

$$n \le j \le 2n \qquad M_j = -P(y_{0j} + y_j) + F_U(l_b + (j-n)\Delta x_L) - F(j-n)\Delta x_L \tag{4}$$

where M_j, y_{0j}, and y_j denote the bending moment, the initial deflection, and the additional deflection caused by

Table 4 Measured Dimensions and Test Results

specimen	Comp. material	Brace material	e [mm]	l [mm]	t [mm]	w [mm]	$\lambda = l/i$	Λ	k_e	P_{max}/P_y	F/P_{max} [%]	F/P_y [%]
E10125		**A**		384.50	15.58	37.73	85.48	1.006	0.96	0.75	0.88	0.66
E10325				383.30	15.62	37.78	84.99	1.001	2.70	0.76	1.71	1.29
E10525		**B**	upper 0.998	382.40	15.63	37.78	84.76	0.998	3.50	0.73	1.66	1.21
E10133		**A**		383.20	15.60	37.81	85.08	1.002	0.86	0.72	1.42	1.02
E10333				383.80	15.60	37.78	85.24	1.004	2.78	0.74	2.00	1.49
E10533		**B**	lower 0.997	383.20	15.64	37.73	84.87	0.999	3.21	0.80	1.91	1.52
E10150		**A**		383.20	15.64	37.93	84.89	1.000	0.99	0.79	1.77	1.39
E10350				383.50	15.60	37.70	85.18	1.003	2.60	0.88	2.27	1.99
E10550		**B**		383.30	15.61	37.77	85.04	1.001	4.02	0.84	3.29	2.77
E15125				574.00	15.63	37.87	127.22	1.498	1.05	0.53	2.71	1.44
E15325				573.90	15.62	37.88	127.24	1.498	2.36	0.54	2.91	1.57
E15525			upper 1.348	573.80	15.63	37.78	127.16	1.497	3.40	0.62	3.00	1.85
E15133				573.60	15.66	37.87	126.89	1.494	0.98	0.63	1.71	1.07
E15333	**A**			574.20	15.62	37.82	127.38	1.500	2.56	0.66	2.62	1.73
E15533			lower 1.354	573.40	15.62	37.90	127.16	1.497	3.71	0.72	2.43	1.75
E15150				574.50	15.63	37.88	127.30	1.499	0.91	0.71	2.28	1.61
E15350				573.50	15.63	37.88	127.11	1.497	2.49	0.81	2.11	1.70
E15550				573.60	15.63	37.93	127.13	1.497	3.17	0.81	2.16	1.74
E20125				765.70	15.61	37.72	169.98	2.001	0.93	0.31	3.63	1.13
E20325				765.00	15.63	37.88	169.57	1.997	2.04	0.37	4.30	1.59
E20525			upper 1.737	765.40	15.59	37.73	170.07	2.003	3.11	0.39	4.11	1.60
E20133				765.80	15.59	37.77	170.17	2.004	0.96	0.40	3.64	1.44
E20333				765.60	15.58	37.78	170.18	2.004	2.39	0.48	3.39	1.63
E20533		**A**	lower 1.740	765.20	15.60	37.85	169.96	2.001	3.36	0.53	3.39	1.78
E20150				764.80	15.61	37.73	169.69	1.998	0.86	0.60	3.14	1.88
E20350				765.70	15.59	37.72	170.12	2.003	1.82	0.70	2.51	1.75
E20550				765.20	15.58	37.73	170.10	2.003	2.48	0.70	3.19	2.23
E24125				1109.70	15.96	37.98	240.83	4.073	0.79	0.09	9.48	0.83
E24325	**C**			1110.00	15.97	38.05	240.76	4.072	2.48	0.11	10.73	1.22
E24525				1109.00	15.95	38.03	240.90	4.075	4.36	0.12	9.76	2.62
E24525'			upper 2.513	1077.20	15.62	38.13	238.94	2.811	3.93	0.28	5.07	1.42
E24133	**B**			1077.00	15.59	38.12	239.37	2.816	1.10	0.25	5.80	1.45
E24333				1076.80	15.62	38.12	238.85	2.810	3.41	0.34	3.64	1.23
E24533				1076.80	15.55	38.08	239.93	2.822	5.47	0.35	3.48	1.23
E24150	**C**		lower 2.497	1109.90	16.02	37.97	240.02	4.060	0.74	0.17	12.34	2.11
E24350				1107.50	15.99	38.07	239.99	4.059	2.48	0.23	3.80	0.88
E24350'	**B**			1078.00	15.51	38.12	240.71	2.832	2.41	0.44	3.58	1.56
E24550	**C**			1109.20	15.95	38.00	240.96	4.076	4.47	0.23	2.08	0.49

e: eccentricity, l: length, t: tchickness, w: width, λ: slenderness ratio, Λ: normalized slenderness ratio, k_e: stiffness parameter, P_{max}/P_y: maximum strength, F/P_{max}, F/P_y: supporting force

loading at the subdivision point j, respectively, and Δx_U and Δx_L the lengths of the subdivided elements of the upper and lower portions, respectively. The central difference expression of the curvature ϕ_j at the point j is given by

$$\phi_j = -y_j'' = -\frac{y_{j+1} - 2y_j + y_{j-1}}{\Delta x^2} \tag{5}$$

where Δx is equal to Δx_U or Δx_L depending on the position of the point j.

The numerical integration scheme to analyze the load-deflection relation is as follows, referring to the flowchart shown in Fig. 5 : First, trial values are assumed for the bending moment at 1st point M_1 and the axial force P for a given value of the displacement y_{given} at the bracing point, and the moment-curvature relation under the axial load P is independently calculated for the cross section of the compression member using the fiber model. Suppose that the integration proceeds to the point j and the quantities M_j, y_j and ϕ_j have been determined at all points from 0 to j. Then, the deflection y_{j+1} at the point $j+1$ is determined from Eq. (5) and then the bending moment M_{j+1} from Eq. (3) or Eq. (4). The curvature ϕ_{j+1} corresponding to M_{j+1} is determined from the moment-curvature relation. After repeating this procedure up to the point n, the bracing point, if the value of the deflection y_n is not sufficiently close to the value of y_{given}, the procedure should be restarted with another trial value of M_1. Otherwise the same procedure is continued up to the point $2n$, the lower support, and if the value of the deflection y_{2n} is sufficiently close to zero, the converged solution is obtained. Otherwise the procedure should be restarted with another trial values of M_1 and P at the beginning. In the numerical calculation, the moment-curvature relation was determined from the mathematically-expressed stress-strain relation obtained by curve-fitting the results of the tensile test shown in Fig. 3. The initial deflection was assumed to be zero. The value of n was taken equal to 100, and the convergence criteria set for y_n and y_{2n} were $|y_n - y_{given}| < y_{given}/500$ and $|y_{2n}| < l/10^6$, respectively.

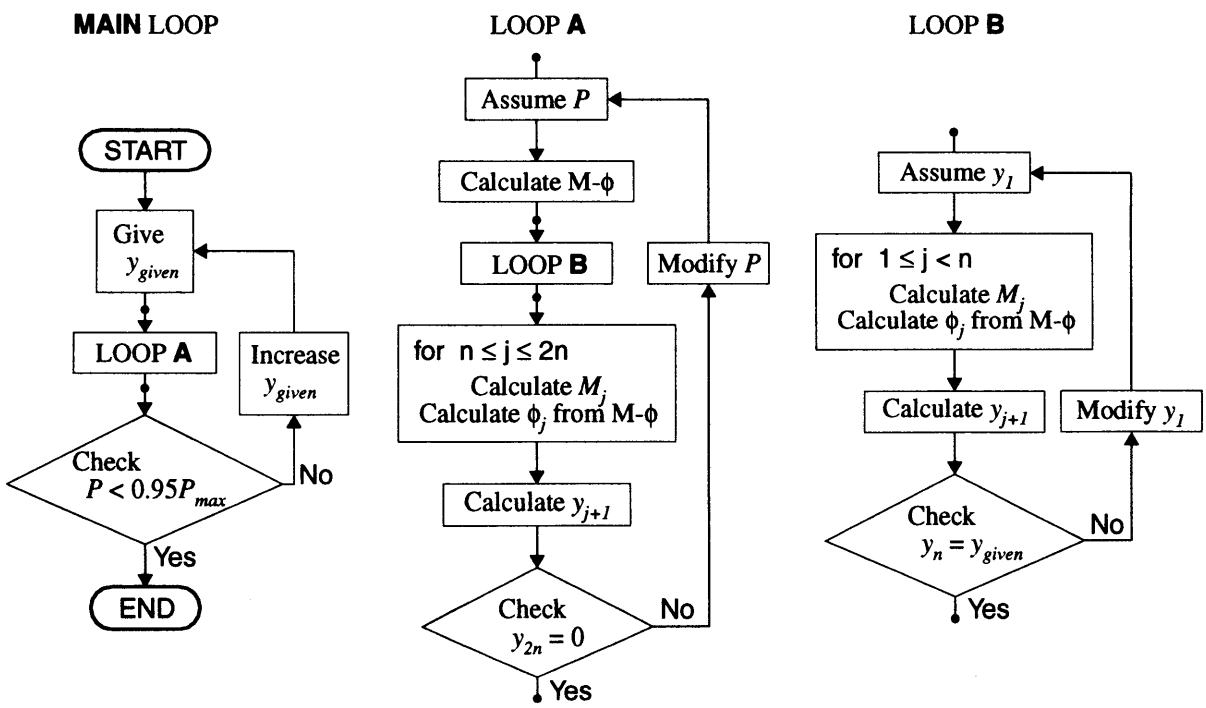

Fig. 5 Flowchart of Analysis

4. Results and discussion

4.1 Load-deflection relations

Non-dimensional load-deflection relations of each specimen are shown in Figs. 6(a)-(d), where the deflections at several points along the length of the specimen are shown, and x denotes the distance from the upper end, and y the lateral deflection. The deflection at the brace is indicated by the black triangle.

The deflection reversal after the maximum load occurred in the specimens braced at midpoint except for the specimen **E15350**. In the case of the specimens with $\Lambda = 2.0$, the shift of the deflection mode occurred, from a half to a full wave of sine curve, right after the yielding started in the compression member, and the compression load suddenly reduced. In the case of specimens with bracing points $l_b / l = 0.25$ and 0.33, the deflection reversal was observed after the load reduced to 80 to 60 % of the maximum load, as the bracing stiffness increased, but its amount was rather small.

Sample results of the analysis are shown in Fig. 7 compared with the test results. In the case of **E15125**, the analysis shows very high accuracy. However, in the case of **E15150** which was braced at the center and involved the deflection reversal, the converged solution could have been obtained only a little after the point of the maximum load. The reason of the non-convergence after the maximum load point is not yet clarified.

4.2 Deflected configurations

Deflected configurations of each specimen at several loading stages are illustrated in Fig. 8(a)-(d). Black

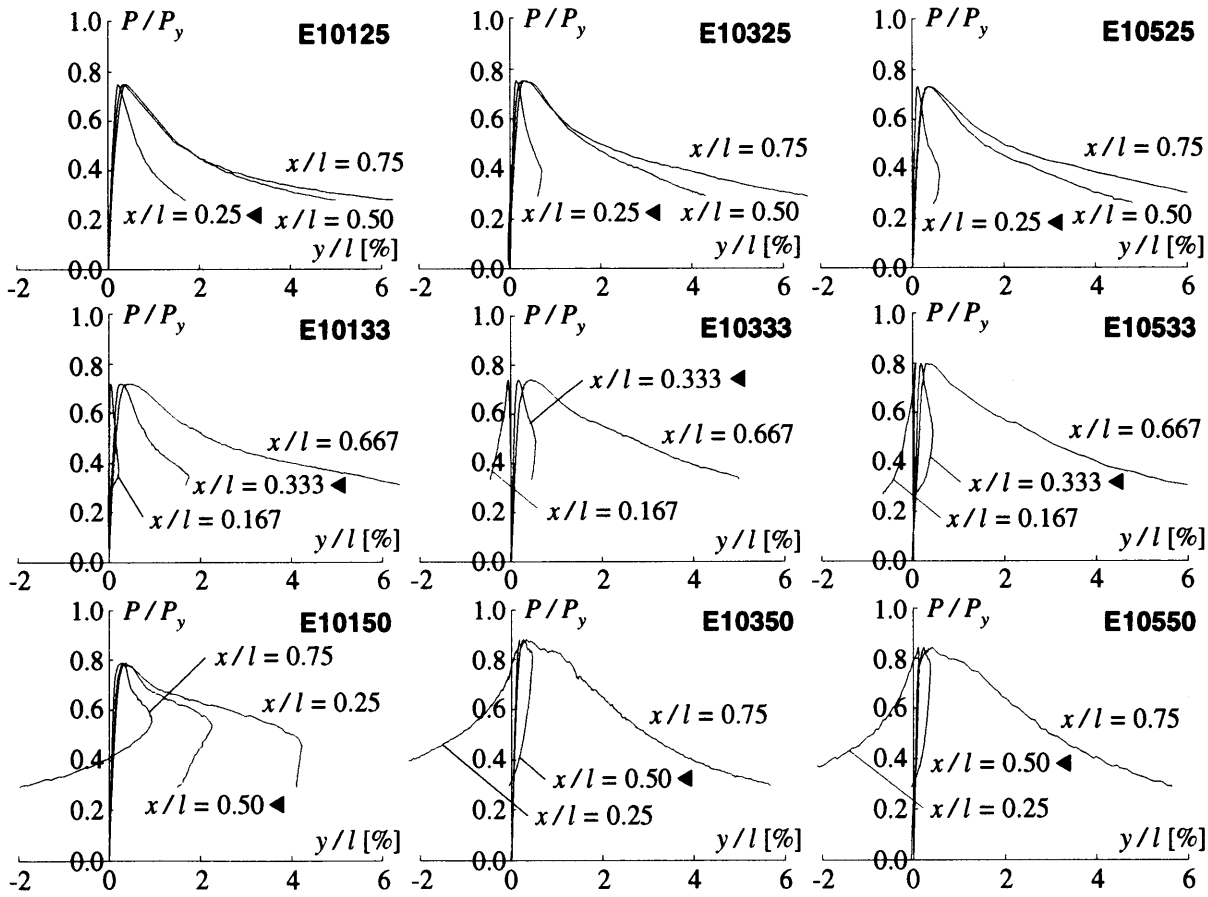

Fig. 6(a) Load-Deflection Relations ($\Lambda = 1.0$)

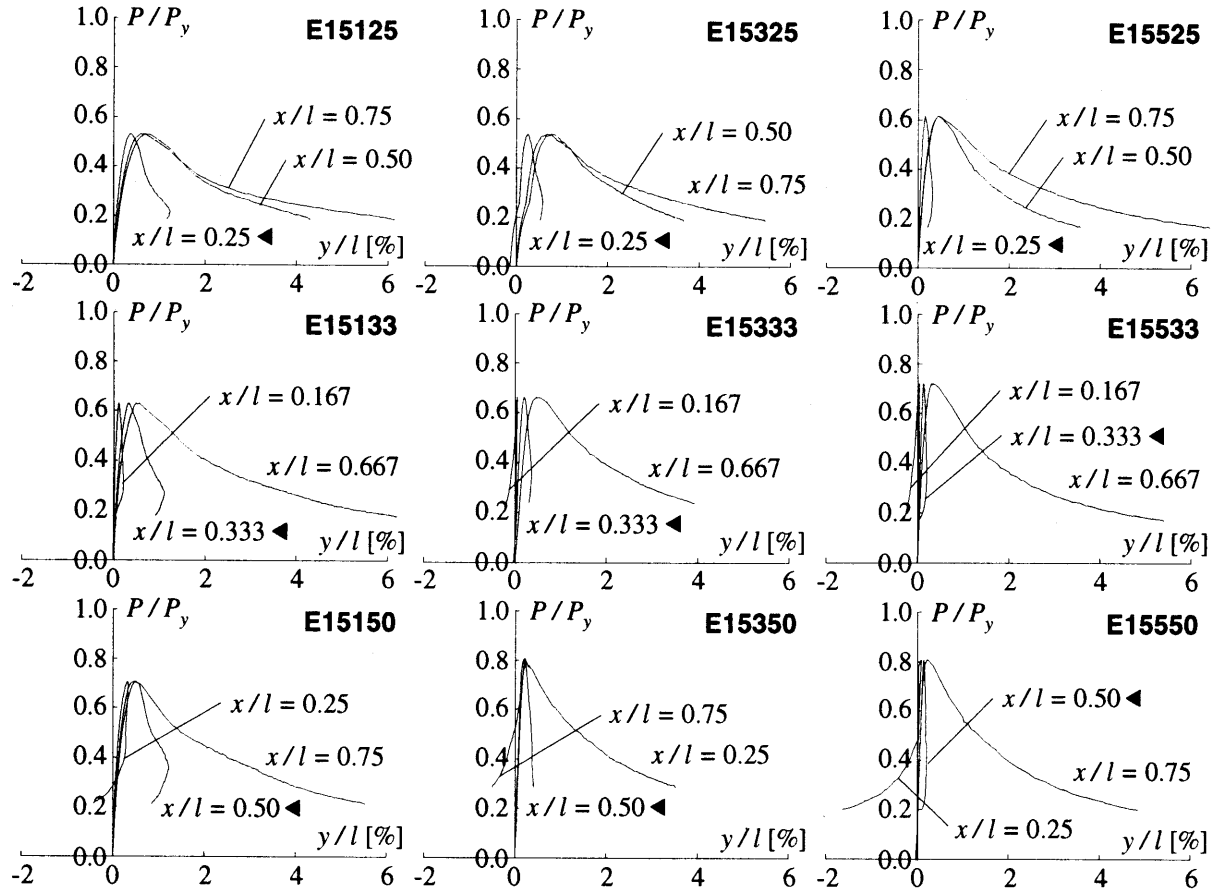

Fig. 6(b) Load-Deflection Relations ($\Lambda = 1.5$)

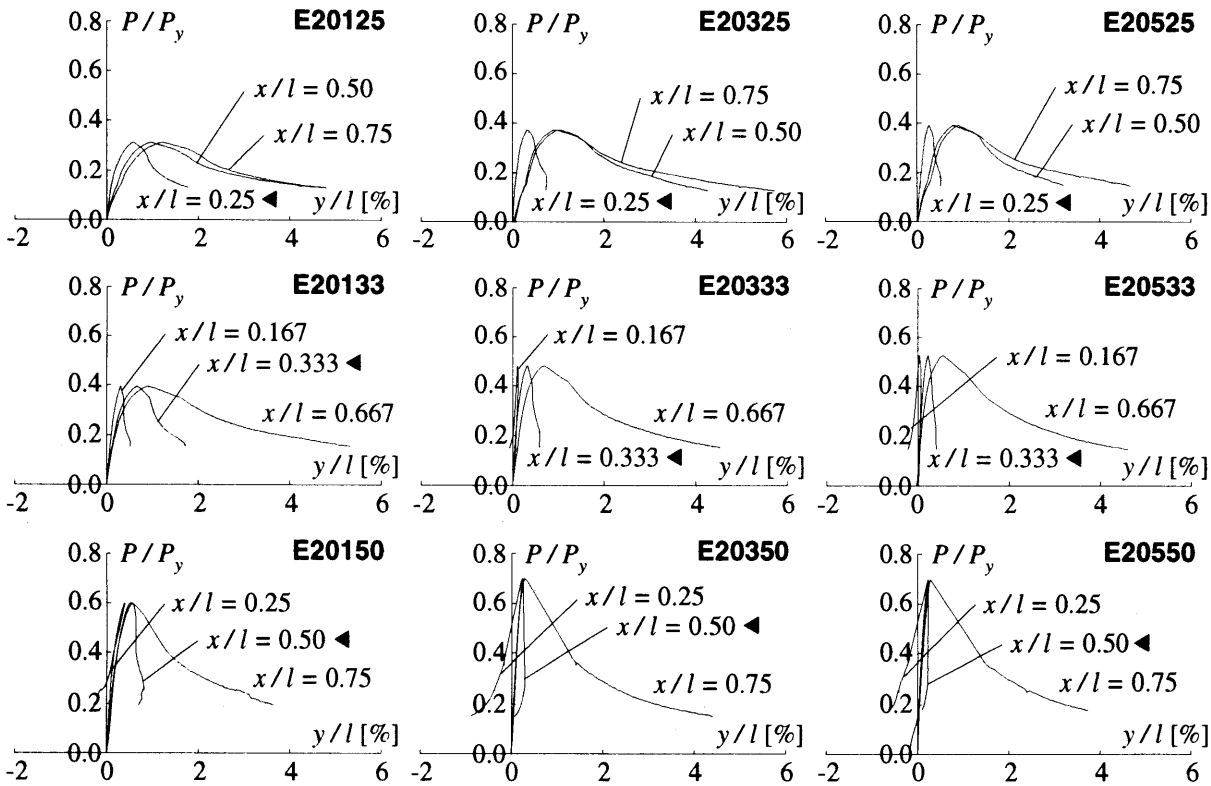

Fig. 6(c) Load-Deflection Relations ($\Lambda = 2.0$)

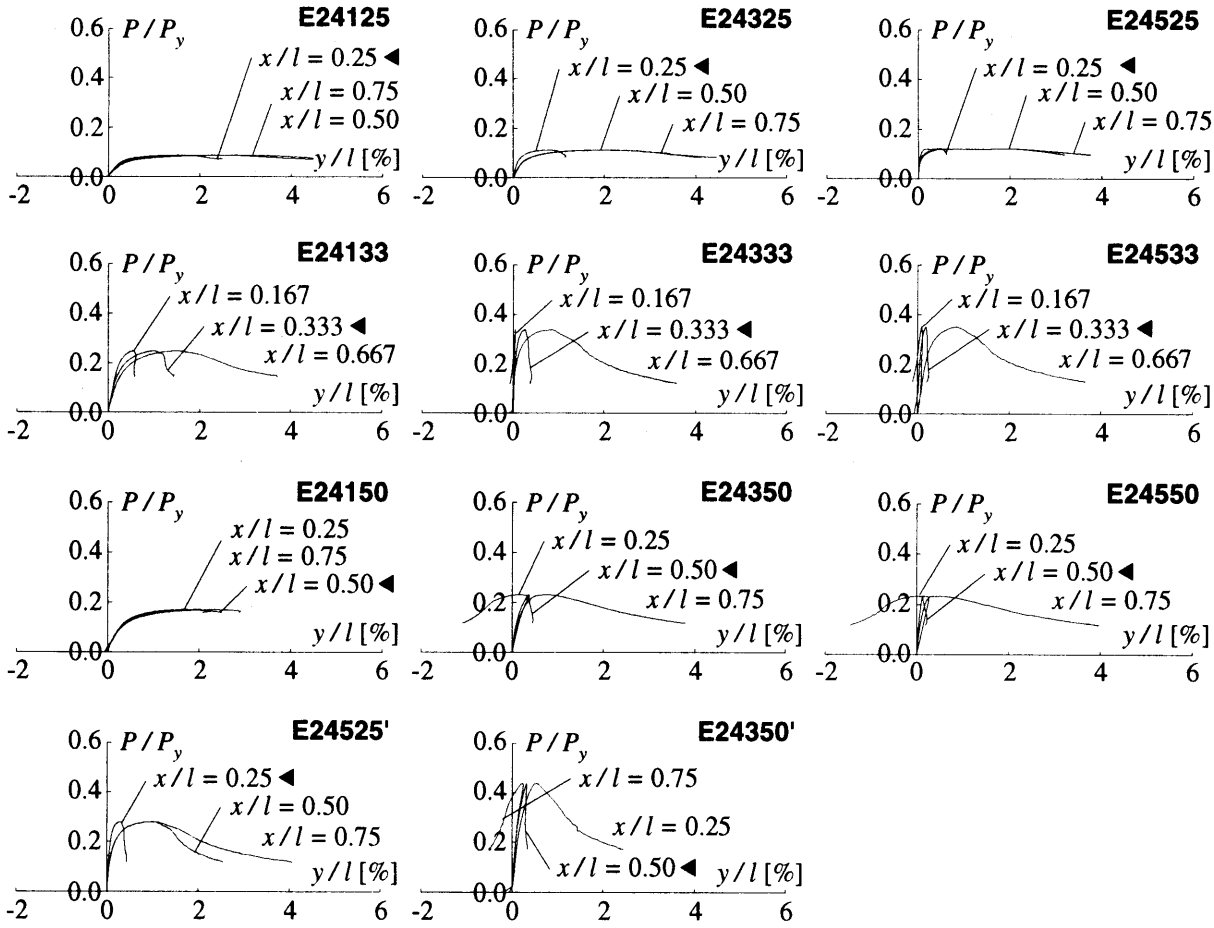

Fig. 6(d) Load-Deflection Relations ($\lambda = 240$)

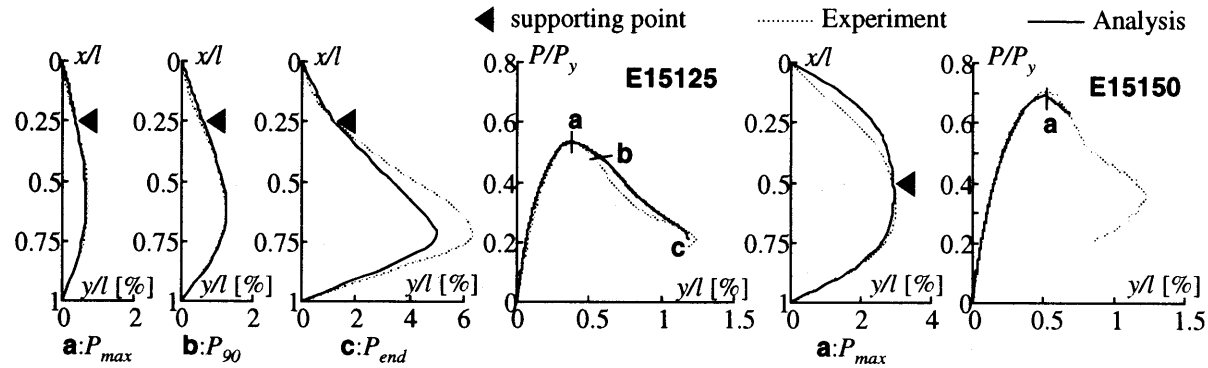

Fig. 7 Comparison between Results of Test and Analysis

triangle indicates the position of the intermediate lateral brace. Each configuration is identified by the loading stage indexes P_{max}, P_{XX}, and P_{end}, which correspond to the loading stages at the maximum load reached, the load reduced to XX% of the maximum load, and the end of the test, respectively.

The shift of the deflection mode from a half to a full wave of sine curve occurred after the maximum load in the specimens braced at midpoint. Especially in the specimens with $\Lambda = 2.0$, a rapid shift of mode occurred right after the yielding started. Only the specimen **E24150** maintained the mode of a half sine wave after the maximum load, but the deflection reached the capacity of the displacement meter, and thus the final mode was not detected. In general, the bracing point deflection at the maximum load became smaller, and the shift of the deflection mode

occurred more clearly, as the bracing stiffness increased. The deflection reversal occurred at the bracing point or at the upper portion higher than the bracing point in some of the specimens with bracing points $l_b / l = 0.25$ and 0.33, but its amount was small and the effect on the mode shift was very little.

Sample results of the analysis are shown in Fig. 7 compared with the test results. As mentioned before, in the case of **E15150**, the converged solution could not have been obtained after the maximum load point.

4.3 Bracing force

The ratio of the bracing force F to the maximum load P_{max} is plotted against the non-dimensional axial load P/P_y in Fig. 9. It is generally observed that the bracing force ratio at the maximum load becomes larger, as the slenderness ratio increases, and as the bracing point parts away from midpoint.

In Fig. 10, the values of F/P_{max} are plotted against the values of k_e, where F/P_{max} indicates the value of the bracing force ratio when the axial load reached the maximum value. The value of F/P_{max} is not much affected by the value of k_e, and it becomes larger as the bracing point parts away from the center, in general. In the conventional design, the bracing force is usually taken equal to 2% of the axial strength of the compression member[7], but the test results show that it was a little larger than 2% even in the case of the specimens braced at the center, since the value of k_e was rather small. In the case of specimens braced at the quarter point, the bracing force ratio does not change much with the change in the bracing stiffness.

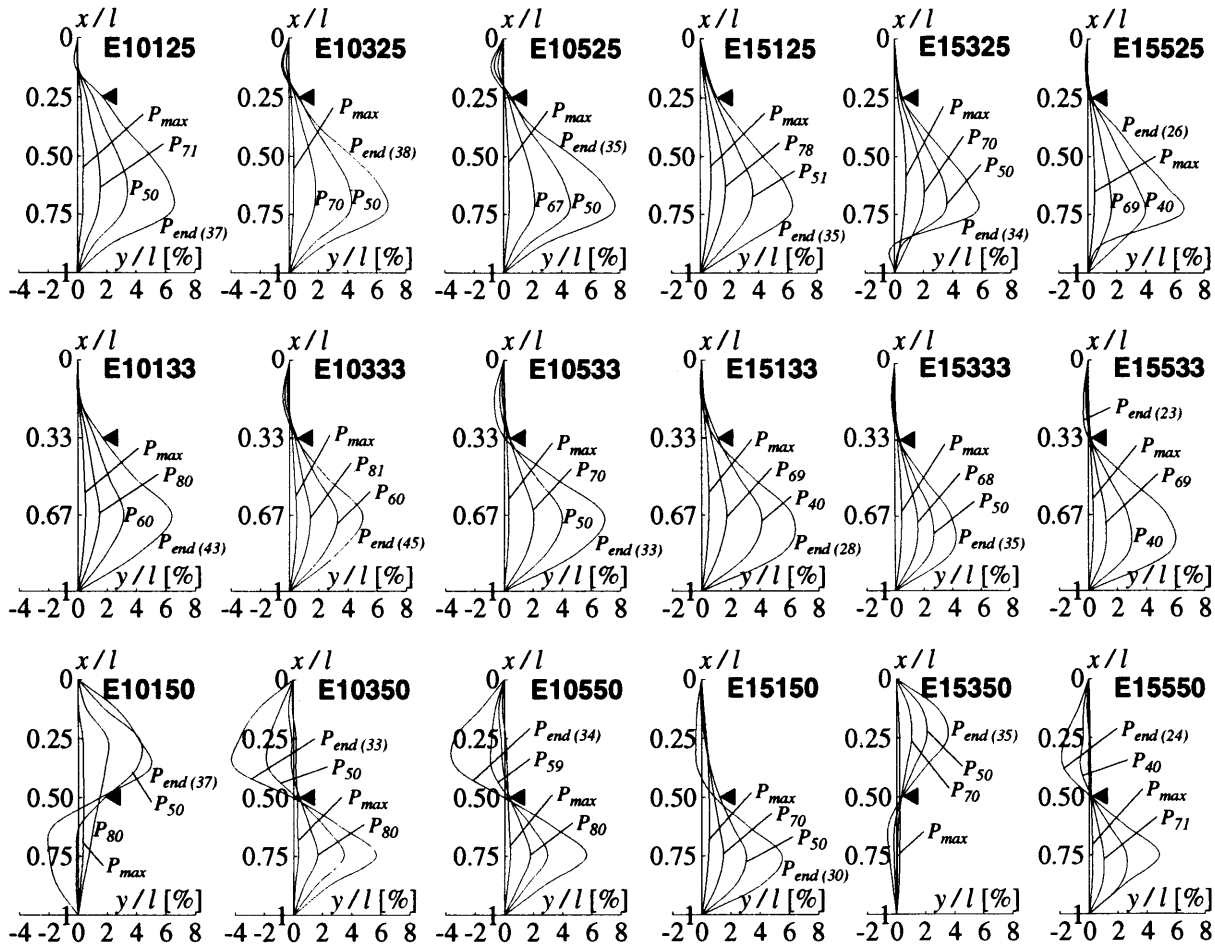

Fig. 8(a) Deflected Configuration ($\Lambda = 1.0$)

Fig. 8(b) Deflected Configuration ($\Lambda = 1.5$)

4.4 Maximum strength

In Fig. 11, the values of the maximum strength P_{max}/P_y obtained from the tests are plotted against the values of Λ_a which is the normalized slenderness ratio calculated for the buckling length equal to l_a (see Fig. 1). The solid line indicates the column curve specified by AIJ Standards for Limit State Design of Steel Structures[9]:

$$\begin{aligned} &\lambda_c \le {}_p\lambda_c && P_c = P_y && ; && {}_p\lambda_c = 0.15 \\ &{}_p\lambda_c < \lambda_c \le {}_e\lambda_c && P_c = \left(1.0 - 0.5\frac{\lambda_c - {}_p\lambda_c}{{}_e\lambda_c - {}_p\lambda_c}\right)P_y && ; && {}_e\lambda_c = 1/\sqrt{0.6} \\ &{}_e\lambda_c < \lambda_c && P_c = \left(\frac{1}{1.2\lambda_c^2}\right)P_y \end{aligned} \qquad (6)$$

The ratios of P_{max} to P_a are listed in Table 5, where P_a is the strength of the centrally-loaded compression member calculated by Eq. (6) taking the buckling length equal to l_a. On the other hand, the values of P_{max}/P_y are plotted against $\Lambda_k = (l_k/i)(\sqrt{\sigma_y/E})/\pi$ in Fig. 12, where l_k is the effective buckling length determined by analyzing the overall elastic buckling strength of the model shown in Fig. 1 with $e = 0$. The slope deflection method derives the buckling condition of this model as follows:

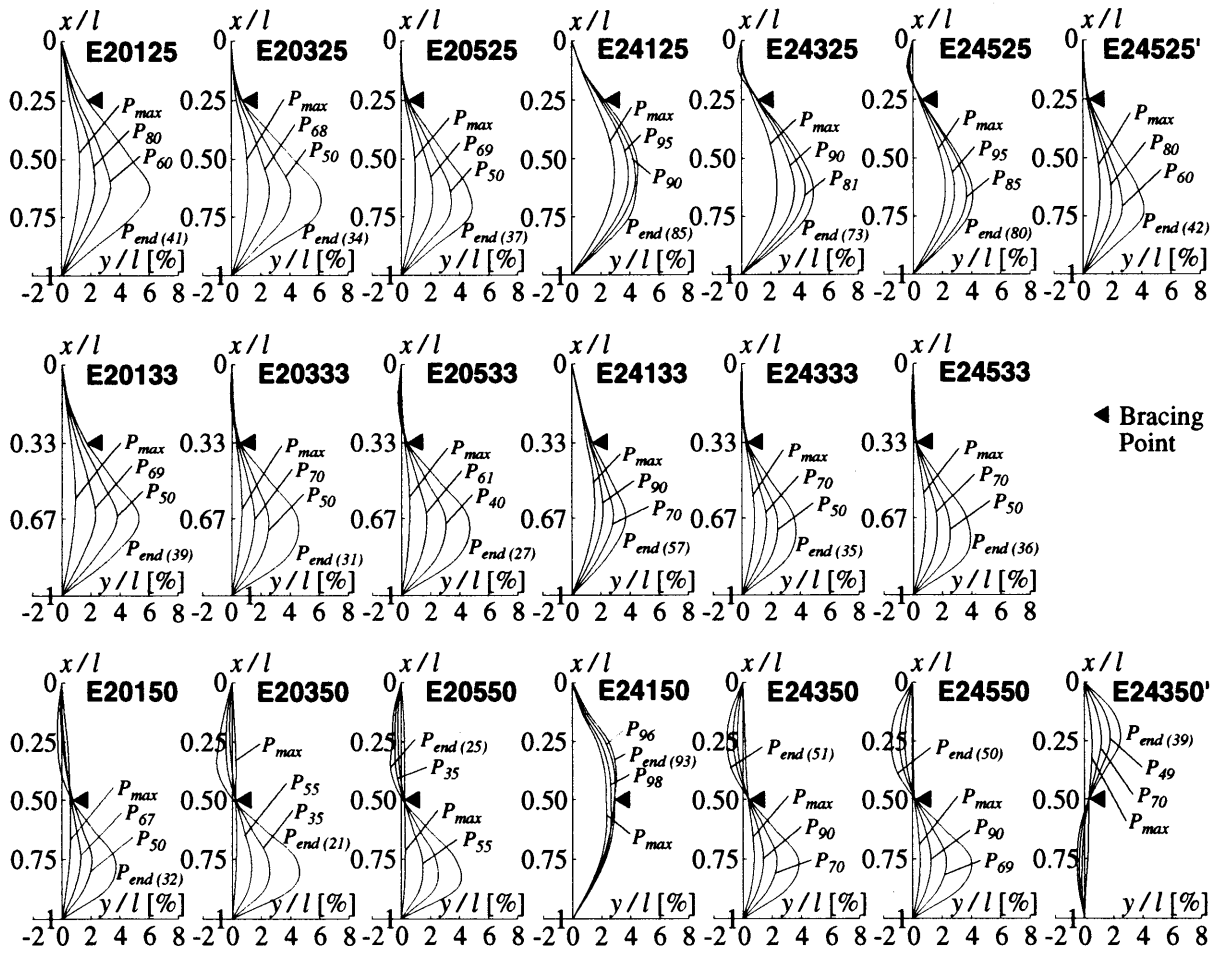

Fig. 8(c) Deflected Configuration ($\Lambda = 2.0$)

Fig. 8(d) Deflected Configuration ($\lambda = 240$)

$$\left(\xi_1 + \frac{l_a}{l_b}\xi_2\right)\left\{\eta_1 + \left(\frac{l_a}{l_b}\right)^3 \eta_2 + \frac{l_a^3 K}{EI}\right\} - \left\{\xi_1 - \left(\frac{l_a}{l_b}\right)^2 \xi_2\right\}^2 = 0 \tag{7}$$

where

$$\xi_i = \frac{Z_i^2 \sin Z_i}{\sin Z_i - Z_i \cos Z_i} \tag{8.1}$$

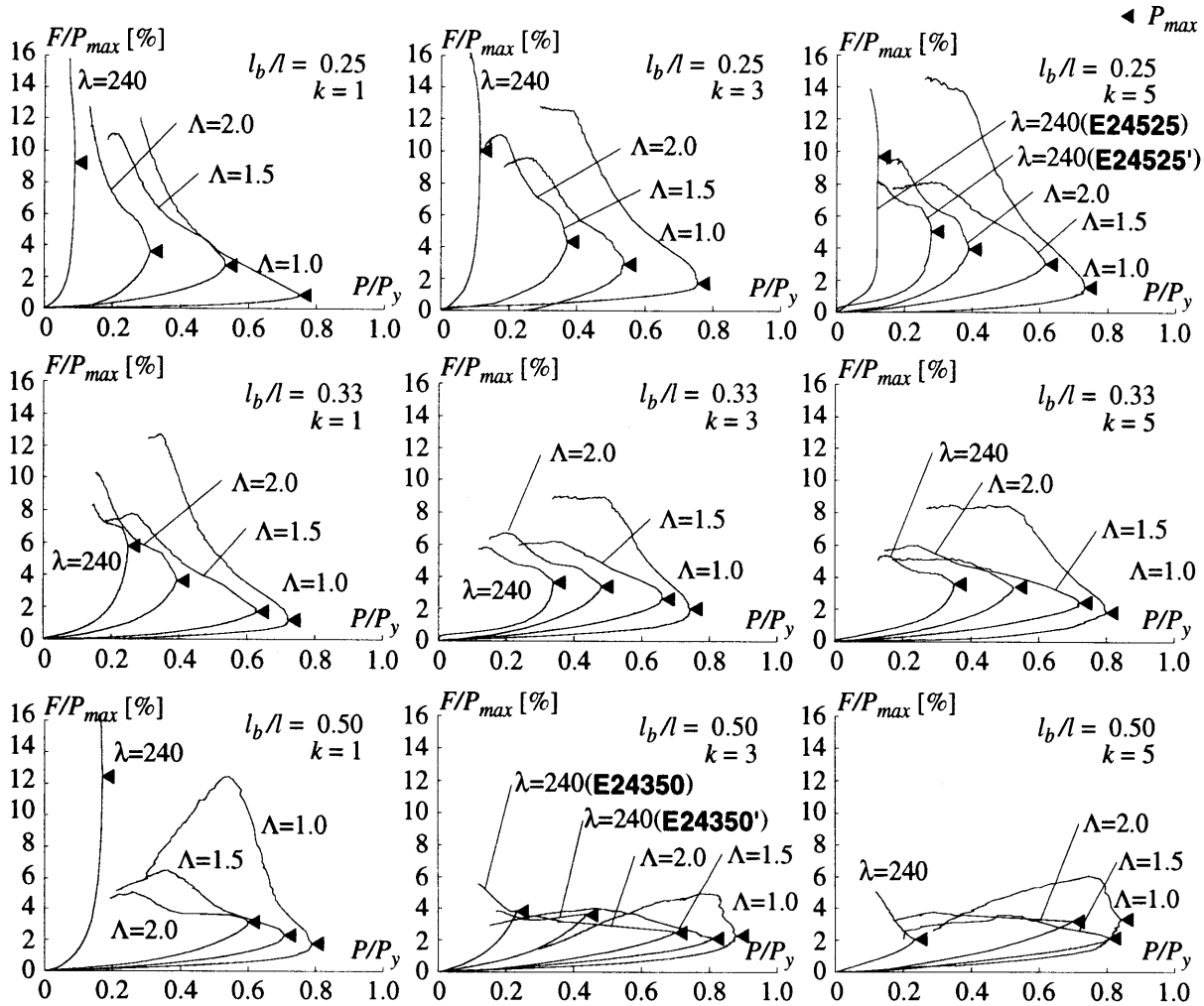

Fig. 9 Relations between F/P_{max} and P/P_y

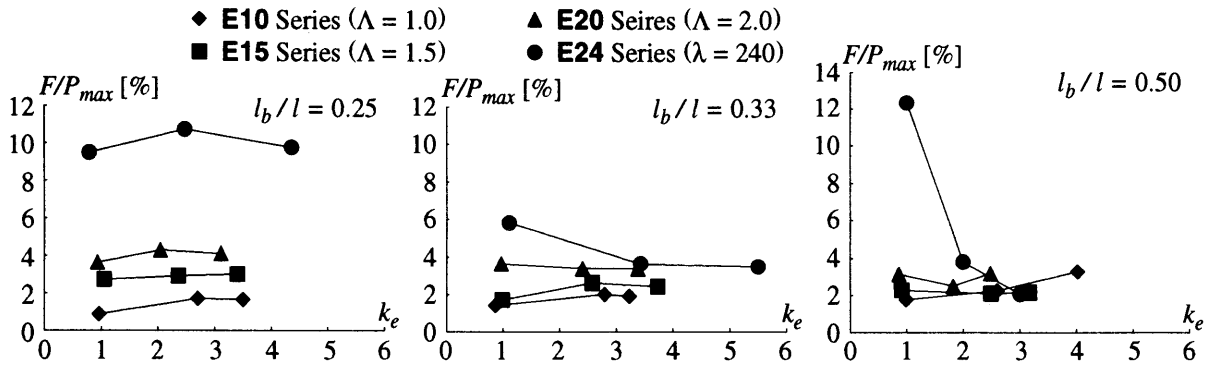

Fig. 10 Relations between F/P_{max} and k_e

$$\eta_i = \frac{Z_i^3 \cos Z_i}{\sin Z_i - Z_i \cos Z_i} \tag{8.2}$$

$$Z_1 = l_a\sqrt{\frac{P}{EI}},\quad Z_2 = l_b\sqrt{\frac{P}{EI}} \tag{8.3}$$

Effective length l_k is obtained by substituting P_{cr}, which is the solution of Eq. (7) for P, into Eq. (9).

$$l_k = \pi\sqrt{EI/P_{cr}} \tag{9}$$

The values of P_{max}/P_k are also listed in Table 5, where P_k is the strength of the centrally-loaded compression member calculated by Eq. (6) taking the buckling length equal to l_k.

The maximum strength of the compression member plotted against the slenderness ratio Λ_a in Fig. 11 exceeds the column strength curve in many cases, while those plotted against Λ_k show a good agreement with the curve given by Eq. (6). It becomes known from Table 5 that the brace works more effectively as the bracing point approaches to midpoint, and as the bracing stiffness increases.

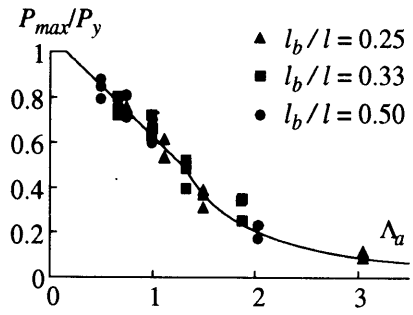

Fig. 11 Relations between P_{max}/P_y and Λ_a

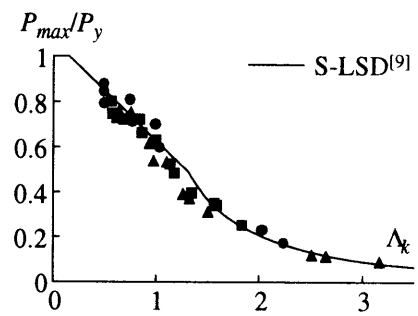

Fig. 12 Relations between P_{max}/P_y and Λ_k

Table 5 Maximum Strength

specimen	k_e	P_{max}/P_a	P_{max}/P_k	specimen	k_e	P_{max}/P_a	P_{max}/P_k
E10125	0.96	1.021	1.024	**E20125**	0.93	0.840	0.849
E10325	2.70	1.025	0.964	**E20325**	2.04	1.006	0.796
E10525	3.50	0.992	0.924	**E20525**	3.11	1.052	0.761
E10133	0.86	0.933	0.892	**E20133**	0.96	0.844	0.870
E10333	2.78	0.962	0.915	**E20333**	2.39	1.023	0.882
E10533	3.21	1.031	0.978	**E20533**	3.36	1.121	0.928
E10150	0.99	0.931	0.931	**E20150**	0.86	0.954	0.984
E10350	2.60	1.040	1.040	**E20350**	1.82	1.115	1.112
E10150	4.02	0.995	0.995	**E20550**	2.48	1.115	1.112
E15125	1.05	0.928	0.918	**E24125**	0.79	0.986	1.064
E15325	2.36	0.940	0.848	**E24325**	2.48	1.276	0.967
E15525	3.40	1.074	0.944	**E24525**	4.36	1.322	0.900
E15133	0.98	1.000	1.002	**E24133**	1.10	1.057	1.021
E15333	2.56	1.055	0.965	**E24333**	3.41	1.428	1.038
E15533	3.71	1.148	1.037	**E24533**	5.47	1.496	1.045
E15150	0.91	0.963	0.977	**E24150**	0.74	0.807	1.032
E15350	2.49	1.095	1.094	**E24350**	2.48	1.090	1.142
E15550	3.17	1.093	1.092	**E24550**	4.47	1.113	1.166
E24525'	3.93	1.493	1.047	**E24350'**	2.41	1.051	1.062

5. Conclusions

38 specimens of the eccentrically-loaded compression member braced at an intermediate point were tested, whose normalized slenderness ratios were 1.0, 1.5, 2.0 and actual slenderness ratio 240, and load eccentricity was taken equal to $i/20 + l/500$. The following phenomena were obtained from the tests.

1. The deflection reversal at the bracing point tended to more clearly appear in the members with longer length, with larger brace stiffness, and braced at the point nearer to the center.
2. The bracing force ratio at the maximum load was not much affected by the brace stiffness, and it became larger as the bracing point parted away from the midpoint, in general, and it became larger than 10% in the case of the specimens braced at the quarter point.
3. The ratio of the maximum load obtained in the test to the calculated strength became larger as the brace stiffness increased and the bracing point approached to the center. The bracing efficiency becomes better as the bracing point approaches to the center.
4. The solution of the analysis, which satisfies the equilibrium at each subdivision point along the member length and determines the deflection based on the moment-curvature relation, very well traced the experimental behavior of the longer specimen with smaller brace stiffness, but the converged solution was obtained only a little after the point of the maximum strength, in the case of some specimens which involved the deflection reversal.

References

[1] Zuk, W., 1956, Lateral Bracing Forces on Beams and Columns, Journal of the Engineering Mechanics Division, Proceedings of the ASCE, Vol. 82, No. EM3, pp. 1032-1 - 1032-11.

[2] Winter, G., 1960, Lateral Bracing of Columns and Beams, Transactions of ASCE, Vol. 125, Part I, pp. 807-845.

[3] Saisho, M., Tanaka, H., Takanashi, K. and Udagawa, K., 1971, Lateral Bracing of Compression Members, Transactions of AIJ, No. 184, pp. 73-79 (in Japanese).

[4] Matsui, C. and Matsumura, H., 1973, Study on Lateral Bracing of Axially Compressed Members (Part 1 and 2), Transactions of AIJ, No. 205, pp. 23-29, and No. 208, pp. 15-21 (in Japanese).

[5] Ono, T., Ishida, T. and Shimono, K., 1995, A Study on Bracing for Steel Column and Beam Considering Limit State, Journal of Structural and Construction Engineering (Transactions of AIJ), No. 469, pp. 117-125 (in Japanese).

[6] Nishino, T. and Tsuji, B., 1996, Behavior of Compression Members with Lateral Bracing, Journal of Structural and Construction Engineering (Transactions of the AIJ), No. 483, pp. 157-163, (in Japanese).

[7] Architectural Institute of Japan, 1973, Design Standard for Steel Structures, Architectural Institute of Japan.

[8] Fukao, H., Morino, S., Kawaguchi, J., 1997, Elasto-plastic Behavior of Laterally-Braced Compression Members, Proceedings of the 5th International Colloquium on Stability and Ductility of Steel Structures, Vol. 1, pp. 499-506.

[9] Architectural Institute of Japan, 1998, Recommendation for Limit State Design of Steel Structures, Architectural Institute of Japan.